Multistatic Multihypothesis Tracking: Environmentally Adaptive and High-precision State Estimates

Martina Daun
Dept. Sensor Data and Information Fusion
FGAN-FKIE
Wachtberg, Germany
Email: daun@fgan.de

Frank Ehlers
System Technology Department
NURC
La Spezia, Italy
Email: ehlers@nurc.nato.int

***Abstract*— Multistatic active sonar has become an important surveillance concept. To fully exploit its benefits in a real-time and realistic scenario, a multihypotheses tracking (MHT) algorithm is proposed which as a extension from standard approaches allows high precision state estimation, treatment of multiple different types of sonar signals and allows adaptation to the highly instationary ocean environment. The algorithm is applied to two data sets gathered at sea trials conducted by NURC, and its performance is compared to the performance of the standard MHT approaches. In particular, the proposed treatment of the Doppler information, exploiting the Doppler notch of the reverberation, similarly to applications in moving target indication for ground surveillance, has led to a large performance gain.**

Keywords: Active Multistatic Sonar, Tracking, MHT, Triangulation, Clutter Notch.

I. Introduction

Multistatic sonar allows a simultaneous look at the target, from several aspects. Because a submarine, which is the target of interest here, is generally designed to be stealth for a monostatic source receiver sonar system, this results in a multistatic sonar system in additional detection opportunities compared to monostatic systems. To exploit this benefit, the association of data gathered at different source receiver pairs is necessary. From a Bayesian perspective, the fusion has to find the "best" combination out of all possible detections from all source-receiver pairs in a batch of a series of measurements. However, for practical solutions the application of the multihypothesis tracking (MHT) scheme has been shown to be sufficient and to solve the data association problem implicitly [9], i.e. following the sequential nature of MHT and updating the underlying tree structure with every new data coming in. When this scheme is applied to real data, however, it becomes obvious that extensions to simple gating and simple approximations of the nonlinear measurement model are necessary. Whilst geometric features of the multistatic measurement can be described deterministically, sonar measurements at sea are stochastic by nature. We propose to extend the standard MHT by two deterministic features:

(i) Incorporation of correct timing that allows the target state estimation at the time when the sound arrives at the target (not at the time when it arrives at a specific receiver, and also not at the time when the active sound signal was transmitted).
(ii) Matched Filter output has a high resolution in time. However, when relative movements between source, target and transmitter exists, Doppler frequency shifts lead to shifts of the correlation maximum in the Matched Filter algorithm. The measurement equation of the Time of Arrival has therefore to be corrected.

The approach to incorporate stochastic knowledge into the tracking and fusion is described by the following steps: modeling the knowledge about the environment by the SONAR Equation, translating this into probability of detection and probability of false alarms used inside the proposed tracking algorithm. However, not only do different geometries occur in a multistatic, but also different types of signals are used: in particular in this paper we study frequency modulated sweeps (FM) and continuous wave signals (CW), which have been transmitted. Thus, in addition to the association necessary to combine data generated by different source receiver pairs, there is also a need to combine data from different "signal channels". Again, although a theoretically optimal approach for this fusion exists in the Bayesian framework [10], for practical considerations, and to result in a real-time capable algorithm, we applied specific techniques (e.g. from ground moving target indication) to combine FM and CW signals and evaluate their performance with the help of data sets from real measurements at sea.

This paper is organized as follows: after this introduction, we will describe the system model and derive the scheme of the standard algorithm in section II. Section III demonstrates the extension of the algorithm with some additional features, and we will discuss our results for two data sets gathered at the NURC sea trials PreDEMUS '06 and SEABAR 07 (NURC's sea trials) in section IV. Section V concludes this paper.

II. Description of the Algorithm

A. Scenario Description

Multihypothesis Tracking (MHT) attracts interest in many applications. Although based on the same idea, quite a large number of different implementations exist. In this work we follow the MHT architecture as described in *Ground target tracking and road map extraction* by Koch et. al [3].
In the application of Active Multistatic Sonar, the state vector is modeled in two-dimensional Cartesian coordinates and we assume a second order movement model

$$\mathbf{x}_k = (\mathbf{p}_k, \dot{\mathbf{p}}_k)^T, \text{ with } \mathbf{p}_k = (x_k, y_k)^T \text{ and } \dot{\mathbf{p}}_k = (\dot{x}_k, \dot{y}_k)^T \tag{1}$$

$$\mathbf{x}_{k+1} = \mathbf{F}_{k+1|k}\mathbf{x}_k + \mathbf{G}_{k+1|k}\mathbf{v}_{k+1}, \tag{2}$$

where $F_{k+1|k}$ and $\mathbf{G}_{k+1|k}$ are matrices and $\mathbf{v}_{k+1}$ is a Gaussian process noise, see [1,4]. Following the NP (Neyman-Pearson) theorem to generate detections, a threshold is applied to the normalized data: given a desired false alarm rate, the system can handle the probability of detection and the threshold is defined. We distinguish between the Detection Threshold (DT) (contacts are considered for updating existing hypotheses) and the Initiation Threshold (IT) (contacts will be considered to initiate a new track).

B. Measurement Model

The measurements are non-linear functions of the target state

$$\mathbf{z}_k = h(\mathbf{x}_k) + \mathbf{w}_k, \tag{3}$$

with Gaussian measurement noise $\mathbf{w}_k$. The FM signal provides measurement of the azimuth angle φ and the Time of Arrival (ToA). We consider here the ToA multiplied by the propagation velocity, which is the bistatic range r . For CW we get additional Doppler information, which is proportional to the bistatic range rate $\dot{r}$. Let us therefore distinguish between the measurement vectors $\mathbf{z}_k^{FM} = (\varphi_k, r_k)^T$ and $\mathbf{z}_k^{CW} = (\varphi_k, r_k, \dot{r}_k)^T$ for FM and CW respectively. Let $\mathbf{p}_k = (x_k, y_k)^T$ be the target position and $s_k = (s_k^x, s_k^y)^T$ and $\mathbf{o}_k = (o_k^x, o_k^y)^T$ the localisation of the source and receiver; then the measurement function can be expressed as

$$\begin{aligned} \varphi_k &= \arctan\left(\frac{x_k - o_k^x}{y_k - o_k^y}\right), \\ r_k &= |\mathbf{p}_k - \mathbf{s}_k| + |\mathbf{p}_k - \mathbf{o}_k|, \\ \dot{r_k} &= \frac{\partial r_k}{\partial t}, \end{aligned} \tag{4}$$

where $|\cdots|$ denotes the Euclidian norm. In multistatics, we obtain contact information of different source receiver pairs (S/R pairs) for the same ping. For track initiation we use Unscented Transform (UT)[3] to build an 2D Cartesian estimate using angle and range information of one S/R pair. Velocity will be initiated with zero mean and appropriate covariance. Each set of contact files (for one source and receiver) is used to update existing hypotheses according to the Unscented Kalman Filter (UKF) update formulas. The update scheme is illustrated in Fig. 1.

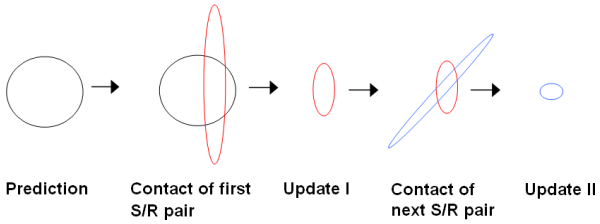

Fig. 1. To illustrate the update scheme we consider contact information of two S/R pairs for the same ping. As a first step, the predicted state estimate is updated with the contact information of the first S/R pair and successively the new state is updated with the contact file of the next S/R pair. The sequence of presenting contacts to the tracking algorithm is arbitrary.

C. Track Extraction and Track Termination

Track extraction as well as track termination is based on sequential likelihood ratio testing. The principle of likelihood ratio testing is briefly summarized in this subsection. We will refer to this summary when extending this principle in the following sections , see [3], [4] for more details.
Given a sequence of measurements $\mathbf{Z}^k = \{\mathbf{z}_1, Z_2, ..., Z_k\}$ with an initial measurement $\mathbf{z}_1$ and Z_i denoting the incoming measurements at time i. The Likelihood Ratio (LR) will be calculated using the hypotheses:
h_1: the data $\mathbf{Z}^k$ contain target measurements and false alarms
h_0: the data $\mathbf{Z}^k$ contain only false alarms
by

$$\mathbf{L}(\mathbf{Z}^k) = \frac{p(\mathbf{Z}^k|h_1)}{p(\mathbf{Z}^k|h_0)} \tag{5}$$

Choosing thresholds A and B , we accept h_1 if $\mathbf{L}(\mathbf{Z}^k) > A$ and h_0 if $\mathbf{L}(\mathbf{Z}^k) < B$. The LR can be recursively calculated summing over all hypotheses weights of the track [4].
Let $\mathbf{H}_k$ denote the interpretation of the track history up to time step k , and e_i^k be the interpretation of the incoming contact information:

$$e_i^k = \begin{cases} \text{contact } i \text{ belongs to the target} & i \neq 0 \\ \text{no detection at time step } k & i = 0 \end{cases} \tag{6}$$

Then the LR can be written as

$$\begin{aligned} \mathbf{L}(\mathbf{Z}^{k+1}) &= \sum_{\mathbf{H}_{k+1}} \frac{p(\mathbf{Z}^{k+1}, \mathbf{H}_{k+1}|h_1)}{p(\mathbf{Z}^{k+1}, \mathbf{H}_{k+1}|h_0)} \\ &= \sum_{\mathbf{H}_k} \sum_{e_i^{k+1}} \lambda_{e_i^{k+1}, \mathbf{H}_k} \frac{p(\mathbf{Z}^k, \mathbf{H}_k|h_1)}{p(\mathbf{Z}^k, \mathbf{H}_k|h_0)} \end{aligned} \tag{7}$$

with

$$\begin{aligned} \lambda_{e_i^{k+1}, \mathbf{H}_k} &= \frac{p(Z_{k+1}, e_i^{k+1}|\mathbf{Z}^k, \mathbf{H}_k, h_1)}{p(Z_{k+1}, e_i^{k+1}|\mathbf{Z}^k, \mathbf{H}_k, h_0)} \\ &= \begin{cases} 1 - P_D & \text{if } i = 0 \\ \dfrac{P_D}{\rho_F}\mathcal{N}(\mathbf{v}_{i,k+1}, \mathbf{S}_{i,k+1}) & \text{if } i \neq 0, \end{cases} \end{aligned} \tag{8}$$

where $\mathcal{N}(\mathbf{v}_{i,k+1}, \mathbf{S}_{i,k+1})$ is the innovation density, which is a result of the Kalman update step at time $k+1$, P_D is the probability of detection and ρ_F the false alarm rate. For track continuation, a two-step procedure has to be followed:

(i) Check for measurements to continue the track. The positive outcome of this check should follow the assumptions about P_D and ρ_F.
(ii) Association of new measurements to track history.

The derivation of the LR assumes well-separated targets and at most one measurement of a target per ping and per each source receiver pair (S/R pair).

III. Extending the Standard Tracking Algorithm

Obviously, a good estimation accuracy is key to a multistatic tracking and fusion algorithm, because the higher this accuracy is, the better the data association will work. Hence, we introduce in subsection A and B two methods, embedded in the MHT framework, to improve estimation accuracy. In subsection C, we explain how the Doppler information extracted from CW echoes is exploited within the MHT algorithm. In subsection D, another extension is proposed that allows the incorporation of a-priori knowledge about the environmental conditions and about the shape of the target.

A. Timing

Due to the rather slow (compared to RADAR application) propagation speed of sound in the water together with the large detection ranges the SONAR system can achieve, it is important to maintain the correct intra-ping timing: This ensures the predicted target state is consistent with the updated one. Assuming target velocity to be constant between two pings, the standard range measurement (4) equation is replaced by

$$r = |\mathbf{p} + t_0\dot{\mathbf{p}} - \mathbf{s}| + |\mathbf{p} + t_0\dot{\mathbf{p}} - \mathbf{o}|, \tag{9}$$

where t_0 is the travelling time of the sound from the source to the target. Let v_s denote the propagation speed of the signal, then we need to solve $\sqrt{(x + t_0\dot{x} - s_1)^2 + (y - t_0\dot{y} - s_2)^2} = t_0 v_s$. Calculations yield

$$t_0 = \frac{z}{2(v_s^2 - v_T^2)} \pm \sqrt{\frac{z^2}{4(v_s^2 - v_T^2)^2} + \frac{r_{ST}}{v_S^2 - v_T^2}}, \tag{10}$$

with $r_{ST} = |\mathbf{p} - \mathbf{s}|$ and $v_T = |\dot{\mathbf{p}}|$. Since $\frac{r_{ST}}{v_S^2 - v_T^2}$ is always the dominating term, the solution with the minus sign can be neglected. We note that for track initiation it is not necessary to consider the timing, since velocity is initiated with zero mean.

B. Doppler Correction for FM

Relative movement between source target and receiver lead to frequency shifts in the received target echo. The Matched Filter converts these frequency shifts into shifts of detection time. Assuming perfect knowledge of the target state, these shifts can be corrected. Equation $f_{max} + t(f_{max} - f_{min}) = f_{max} + \Delta f$ delivers the time shift $t = \frac{\Delta f}{f_{max} - f_{min}}$.
The new measurement equation for range is therefore given by:

$$r = |\mathbf{p} - \mathbf{s}| + |\mathbf{p} - \mathbf{r}| + \frac{\dot{r}}{2}\frac{f_{max} + f_{min}}{f_{max} - f_{min}} \tag{11}$$

Both corrections (the correction for timing (III-A) and the compensation of Doppler shifts described here) are applied in the algorithms.

C. Processing of CW Contacts

During the experiments, FM and CW signals were transmitted. The two waveforms differ in some aspects. Whilst with FM a good range resolution is obtained, the CW delivers additional Doppler information. To fuse information of the two waveforms, it is necessary to bear in mind their characteristics. Due to the poor resolution in range, we decided that CW contacts will not be used for track initialisation.
Furthermore, we will model the probability of detection (P_D) of CW as a function of the measured Doppler value [6]. If the Doppler of the target is close to the Doppler of the background, the target is in the so called Clutter notch and the probability of detection is low; The eventuality that target is in Clutter Notch does not only concern non-moving targets, but may also appear due to geometrical reasons [7]. Let $\dot{r}_T$ be the range rate of the target and $\dot{r}_C$ the range rate of the corresponding background. Using the modeling assumption in [6], we express the P_D depending on the distance $n_c(\mathbf{x}) = |\dot{r}_t - \dot{r}_C|$, on a characteristic sensor information, the minimum detectable velocity (MDV), and a fixed part p_D (this part can also be chosen to be variable with the SNR) :

$$\begin{aligned} P_D(\mathbf{x}) &= p_D\left[1 - \exp\left(-\ln 2\left(\frac{|\dot{r}_T - \dot{r}_C|}{MDV}\right)^2\right)\right] \\ &= p_D\left(1 - \frac{MDV}{\sqrt{\ln(2)/\pi}}\right)\mathcal{N}\left(0; n_C(\mathbf{x}), \frac{MDV^2}{2\ln(2)}\right) \end{aligned} \tag{12}$$

We distinguish between the following approaches:

(i) Use CW measurements to weight hypotheses
Doppler Weighting Method -DoWg
(ii) Use CW measurements for hypotheses update
Doppler Update Method -DoUp
This Method is implemented in analogy to [6]

Ad (i): CW contacts are only used to weight existing hypotheses and do not generate new hypotheses. So, we can choose a low detection threshold for CW contacts, without increasing computational complexity in the following time stages. However, the gain of using the CW signal depends on a good localisation due to FM.
The new weights of the hypothesis tree after processing a set of new CW contacts Z_s^{CW} are calculated by multiplying the added weights for all interpretation possibilities (8).

$$\begin{aligned} &p(Z_s^{CW}, \mathbf{Z}^k|\mathbf{H}_k, h_1) \\ &= p(\mathbf{Z}^k|\mathbf{H}_k, h_1)\sum_{e_i^{s,CW}} p(Z_s^{CW}, e_i^{s,CW}|\mathbf{Z}^k, \mathbf{H}_k, h_1), \end{aligned} \tag{13}$$

where $\mathbf{Z}^k$ denotes the collection of FM and CW measurements up to ping k and $e_i^{s,CW}$ denote the interpretation of contact i or that there is no target contact ($i = 0$).

As part of the Likelihood function we calculate:

$$\begin{aligned} & p(e_i^{s,CW}|\mathbf{H}_k, h_1) = \int p(e_i^{s,CW}, \mathbf{x}_s|\mathbf{H}_k, h_1) d\mathbf{x}_s \\ & = \int p(e_i^{s,CW}|\mathbf{x}_s, \mathbf{H}_k, h_1) p(\mathbf{x}_s|\mathbf{H}_k, h_1) d\mathbf{x}_s \\ & \propto \int \mathcal{N}\left(0; n_C(\mathbf{x}_s), \frac{MDV^2}{2\ln(2)}\right) \mathcal{N}(\mathbf{x}_s; \mathbf{x}_{s|k}, \mathbf{P}_{s,k}) d\mathbf{x}_s \\ & \approx \quad \mathcal{N}\left(0; N_C \mathbf{x}_{s|k}, \frac{MDV^2}{2\ln(2)} + N_C \mathbf{P}_{s|k} N_C^T\right) \end{aligned} \tag{14}$$

The proportionality in the third line is caused by expanding a factor, which only depends on the number of incoming measurements and the sensor parameter MDV; therefore it is independent from the target state $\mathbf{x}_s$. From line three to four, we also use the product formula for Gaussian densities and a approximation by linearization of n_C, with the Jacobian matrix N_C. Again linearization was replaced by UT in the algorithm. The derivation shows that only the predicted state estimate and state covariance influences the considered probability of detection.

Ad (ii): In comparison to the first mentioned method the Doppler Update method processes incoming CW contacts similarly to FM contacts. But again, we need to take care of the modeling assumption for the P_D (12). The update formulas are derived according to the Bayes formalism in [6]. As it can be seen in (12) the fictious 'measurement', the target is in Clutter Notch, is Gaussian distributed due to the modeling assumptions and can therefore processed as an additional 'measurement' information.

D. Environmentally Adaptive Tracking

Until now the probability of detection for FM (and partially also for the CW) was modeled to be uniformly distributed in the observation area. In the derivation of the Likelihood function (8), we have seen that the parameters P_D and ρ_F influence track extraction and track maintenance. The presented approach is especially sensitive with respect to the modeling assumptions, since at each tracking stage information of different S/R pairs is fused. For example, if the target is in a geometrical region where one source receiver pair omits detection, the assumption of uniformly distributed P_D may prevent the track from being extracted. To fix the problem we propose to introduce a variable P_D, which is estimated from the Signal to Noise Ratio (SNR) of a potential contact. Therefore we need to derive the SNR in dependence of the predicted target state.

1) SONAR equation: The SONAR equation combines in logarithmic units (i.e., units of decibels relative to the standard reference of energy flux density of rms pressure of $1\mu Pa$ integrated over a period of one second), the following terms:

$$(S - TL) - (N - AG) - DT \geq 0 \tag{15}$$

which define signal excess where:

- S source energy flux density at a range of 1 m from the source;
- TL propagation loss for the range separating the source and the sonar array receiver;
- N noise energy flux density at the receiving array
- AG array gain that provides a quantitative measure of the coherence of the signal of interest with respect to the coherence of the noise across the receiving array;
- DT detection threshold associated with the decision process that defines the SNR at the receiver input required for a specified probability of detection and false alarm.

For the description of active sonar, the SONAR equation has to be applied for the sound path from the source to the target where the received level plus the target strength (TS) is reflected to the receiver. Also important in the active scenario is that the target echo has to be compared not only to the surrounding noise level but also to the surrounding reverberation level (RL).

Especially interesting with respect to target tracking are these parts of the SONAR Equation, which depend on the target position (TL,TS,NL,RL) and target velocity (TS).

2) Estimating the P_D in terms of the SONAR Equation: The SONAR Equation describes the functional relationship of the SNR of a measurement and the corresponding target state $\mathbf{x}$. In the following we use the function $snr = h(\mathbf{x})$ to formulate the dependency. We assume the SNR to be normal distributed with variance σ_{dB} , which is also assumed to be the variance of the noise level [1]. The probability of detection $P_D(\mathbf{x}, DT)$ and false alarm rate $\rho_F(DT)$ are obtained by integration:

$$\begin{aligned} P_D(\mathbf{x}, DT) &= p(h(\mathbf{x}) > DT) \\ &= \int_{t=DT}^{\infty} \mathcal{N}(t; h(\mathbf{x}), \sigma_{dB}^2) dt \end{aligned} \tag{16}$$

$$\rho_F(DT) = \int_{t=DT}^{\infty} \mathcal{N}(t; 0, \sigma_{dB}^2) dt \tag{17}$$

As a part of the LR we calculate in analogy to (14):

$$\begin{aligned} & p(e_i^k|\mathbf{H}_{k-1}, h_1) \\ & \propto \int \int_{t=DT}^{\infty} \mathcal{N}(t, h(\mathbf{x}_k), \sigma_{dB}^2) dt \mathcal{N}(\mathbf{x}_k; \mathbf{x}_{k|k-1}, \mathbf{P}_{k|k-1}) d\mathbf{x}_k \\ & \approx \int_{t=DT}^{\infty} \mathcal{N}(t, \mathbf{H}\mathbf{x}_{k|k-1}, \sigma_{dB}^2 + \mathbf{H}\mathbf{P}_{k|k+1} H^T) dt, \end{aligned} \tag{18}$$

where $\mathbf{H}$ is the Jacobian of the function h and e_i^k again the interpretation of the contact i or of a missed detection if $i = 0$. Derivations show that the probability of detection depends on the expected SNR and also on the estimation accuracy in this SNR, which obviously depends on the accuracy in the position and velocity estimate. If no knowledge is assumed about the target state the P_D will be about 0.5, which is also the value for the fixed P_D chosen in the standard approaches.

Noise measurements in each bearing and for each receiver and the output of target strength and propagation loss modeling software are used to calculate the actual value of h(x). By using the UT instead of linearization, we do not need to look deeper in the function itself (by calculating derivatives); we can easily process foreign algorithms or even tabular entries.

IV. Data Analysis

In the course of NURC's project on deployable multistatic active sonar, two major sea trials were conducted: PreDEMUS'06 and SEABAR 07. The setup of NURC's deployable equipment (called DEMUS) was different in both sea trials: In the data set selected from PreDEMUS'06, a single source and three receivers were installed, see Fig. 2. The source was operating at low source level, avoiding reverberation and allowing the signal, electronically time shifted and repeated, generated by the Echo Repeater (E/R) towing vessel, to be detected in a more or less stationary noise background. We will call this data set from PreDEMUS'06 "B01" in the following text. The data set selected from SEABAR 07 was generated

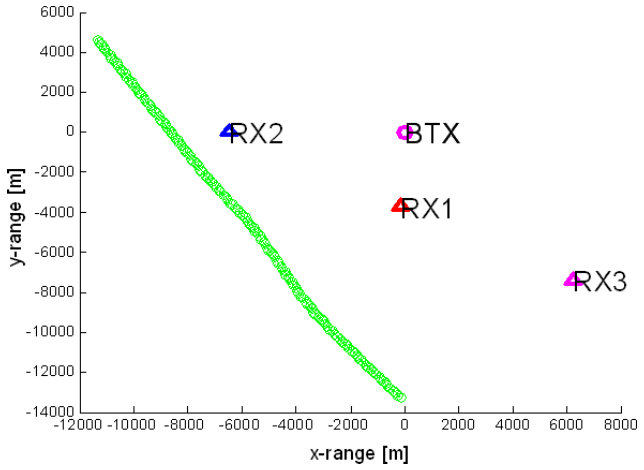

Fig. 2. Plan of B01 in 2D Cartesian; three receiver (RX1, RX2 and RX3) and one source (BTX), the target starts from north-west (green)

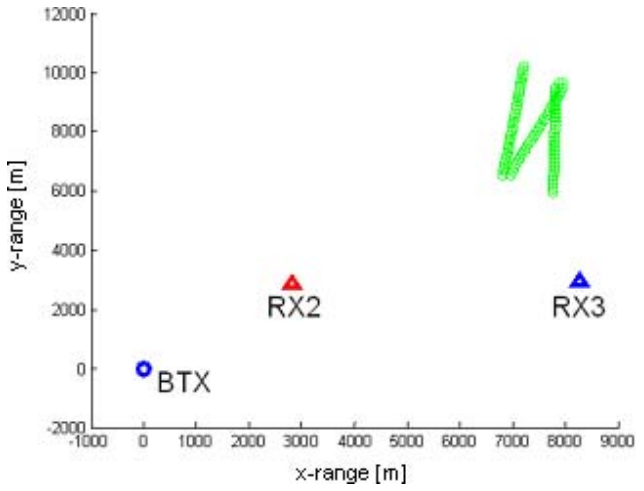

Fig. 3. Plan of A01 transformed in 2D Cartesian; two receivers (RX2 and RX3) and one source (BTX); the target is moving zigzag (green)

by a source operating at full power, thus causing reverberation, and two receivers, see Fig. 3. We will call this data set "A01". In addition to the clutter targets that the reverberation were generating, this data set has another complication caused by very instationary and directional noise. This noise was generated by fast-moving vessels passing the receivers in close vicinity. The setting of the E/R was similar to the setting in B01.

In the following, we will assess the performance of the proposed extensions by applying the algorithms to both data sets. Changes in performance should be made visible when calculating measures like track duration, track fragmentation, latency and number of false tracks. Because just two data sets cannot lead to a sufficient statistical treatment, we focus our discussion of the results on identifying major trends only.

A. Run B01

In B01, the target starts from north-west, see Fig. 2. We choose a detection and initiation threshold of 10dB for FM and no threshold for CW. The corresponding input files for each source receiver (S/R) pair contain about 60 contacts per ping for the FM and about 90 contacts per ping for the CW. Fig. 4 shows the SNRs of the associated target contacts. The three rows include the SNRs for the FM and CW signal obtained by receiver RX1, RX2 and RX3. The distance between the target and the receivers, RX1 and RX3, in the beginning, see Fig. 2, results in low SNRs and a large number of missed detections. Close to ping 30, detection was missed for all three receivers. But after that the probability of detection is quite good.

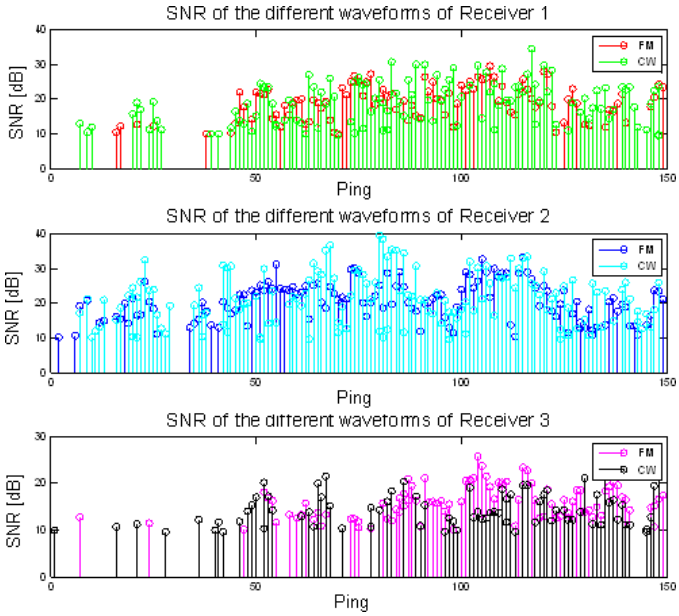

Fig. 4. SNR of target contacts for RX1, RX2 and RX3 respectively; SNR of FM and CW are shown in different colours.

For environmentally adaptive tracking we need to model the SNR values with the help of the SONAR equation. Values for TL and NL were adapted for each receiver from ping to ping. Since an E/R does not have aspect-dependent target strength, the TS value was kept constant. Fig. 5 shows the modeled SNRs calculated from the known position of the target. Model results explain why missed detections occur at the beginning of the RUN. For this run, a very exact ground truth is available

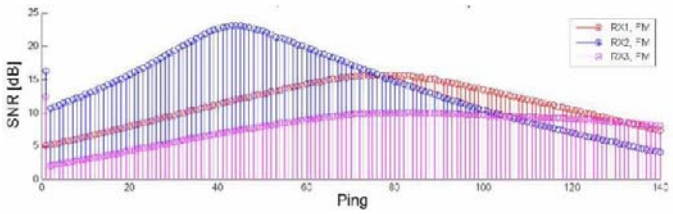

Fig. 5. modeled SNR (FM) for RX1 (red), RX2 (blue) and RX3 (magenta); calculated from the truth

[8]; this gives us the opertunity to analyze the estimation performance.

B. Run A01

In A01 the target is moving zigzag, see Fig.3. In Fig. 6 the SNRs for the target measurements of RX2 and RX3 are shown; again the DT and IT for each S/R pair is 10dB for FM and there is no threshold for CW. The P_D is high for the whole run. We only note some missed detections for RX3 close to ping 40. The Input files for the tracker contain about 150 contacts per ping for the FM and about 100 contacts for the CW. Once E/R detections are uniquely identified, it is possible

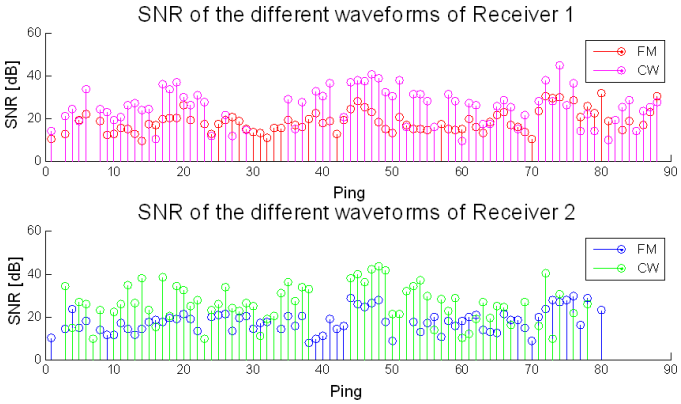

Fig. 6. SNR of target contacts for RX2 and RX3 respectively; SNR of FM and CW are shown in different colors.

to modify their SNR. Fig. 7 shows modified SNRs for the target contacts, calculated by Doug Grimmet, which are about 10dB lower than the original ones, whilst the SNR of the non-target contacts was retained. Of course, this data set is more realistical than the original, but also more challenging with regard to target tracking. Choosing the same DTs as before would cause in a poor P_D for the whole run. So we choose two different thresholds, a detection threshold (DT) of 2dB for FM and CW contacts and an initiation threshold (IT) of 10dB for FM. In this case, the tracker has to process about 500 contacts per ping and each S/R pair for the FM and again about 100 contacts for the CW. However, also in this case we look at a still optimistic scenario, it is questionable whether 2dB is a realistic threshold to form a contact. To model the SNRs for the modified data set, we use the Transmission Loss and Noise Level calculated for this run. The values are given by tabular entries dependent on a distance and angular information. Again

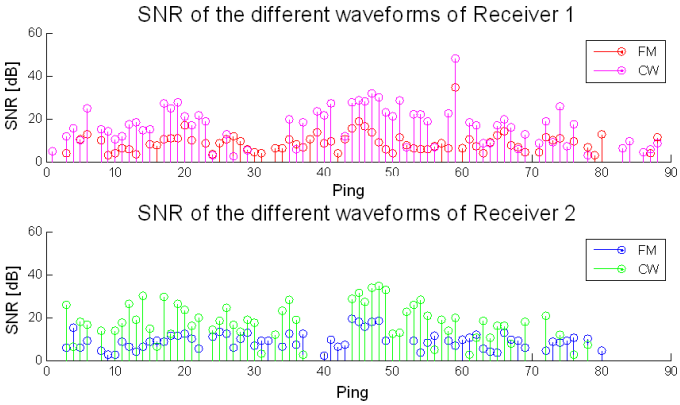

Fig. 7. Modified SNR of target contacts for RX2 and RX3 respectively; SNR of FM and CW are shown in different colours.

the target strength is assumed to be fixed.
The modeled SNRs are shown in Fig. 8. We use the tracking results to illustrate the modeling, since the truth of the target is not available. The missed detections close to ping 40, can be explained by some noise affecting RX3.

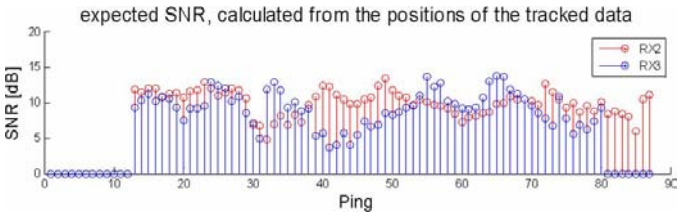

Fig. 8. modeled SNR (FM) for RX2 (red) and RX3 (blue); calculated from the tracking result

C. Results for Timing and Doppler Correction

To demonstrate the increase in accuracy, we apply four "procedures" to calculate the ToA for FM contacts: Doppler Correction (DoCor), Timing (TiCor), Doppler Correction and Timing (DoTiCor) and no correction (NoCor). To understand the effect of the Doppler Correction, we examine the tracking results in detail, see Fig. 10. The truth is marked by green circles; the DoTiCor tracking results is given by blue circles and NoCor by black plus signs. Results for Doppler Correction are shifted at the line; this reflects a bias in the range measurement due to the frequency shift. Now they match the real postions of the E/R source. The data from A01 have been analyzed during the experiment at sea. Hence, only positional information about the E/R towing vessel was available at that time and a detailed post-analysis step to determine the exact position of the E/R sound source (as was accomplished for the B01 data set) was missing. So, we have to compare our results with the position of the towing ship and calculation of the estimation error is not possible. Fig. 10 illustrates the results for DoTiCor and NoCor. Again we note that the result of DoTiCor has shifted with respect to NoCor at the line. At the first maneuver, we observe that the DoTiCor is less robust against deviations from the motion model. This is a

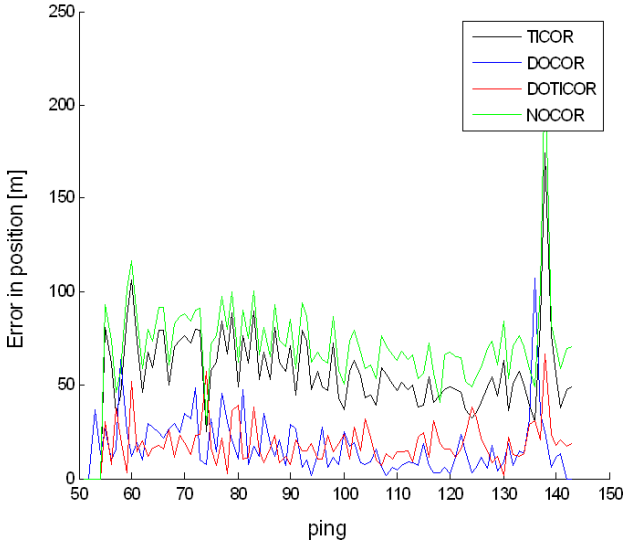

Fig. 9. Estimation error for tracking results of B01 using approaches TiCor and DoCor

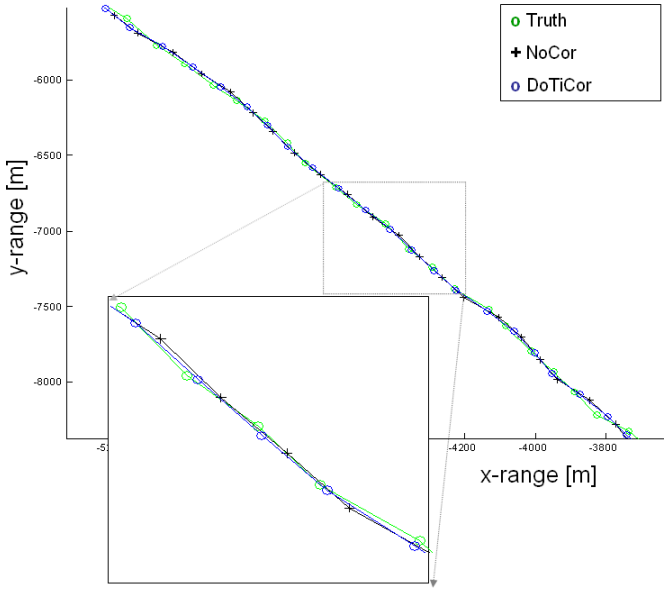

Fig. 10. Tracking results of B01 for NoCor and DoTiCor. The position of the E/R is shown in green.

consequence of the influence that the estimated Doppler has on the range measurement.

Table 1 and 2 show the start, the end of the track and the total number of tracks that has been extracted during the whole run. For both runs the latency, which is the time the tracker needs to decide that threre is a target, and the number of false tracks could be slightly reduced with DoTiCor. But statistics are not sufficient to note trends.

D. Results for using also CW measurements

In this part we analyze the results for using the additional CW measurements for weighting hypotheses (DoWg) or for using them for hypothesis update (DoUp). Table 3 and 4

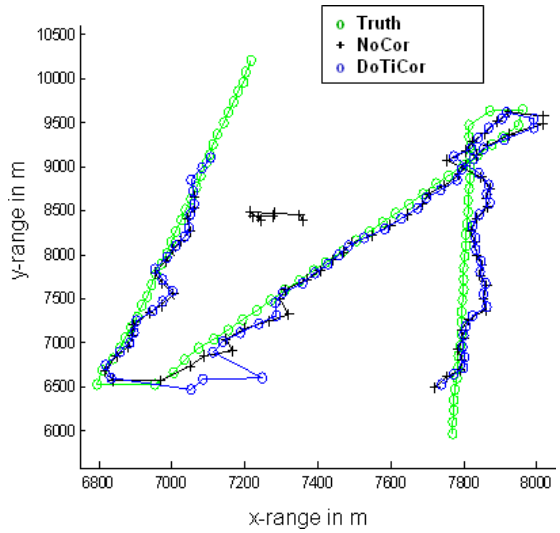

Fig. 11. Tracking results of A01 for NoCor and DoTiCor. The position of the towing ship is shown in green. Distances in [m]

TABLE 1
DoTiCor - Tracking results for B01

	Start of track [ping]	End of track [ping]	Total Number of tracks
FM NoCor	54	146	66
FM DoTiCor	53	146	63

TABLE 2
DoTiCor - Tracking results for A01

	Start of track [ping]	End of track [ping]	Total Number of tracks
FM NoCor	15	88	69
FM DoTiCor	12	88	58

point out the results in terms of track duration, track latency and the number of false tracks compared with the standard tracking results using only FM. The number of false tracks can be reduced, due to the additional contact information. As foreseen, the two data sets do not deliver sufficient statistics to rank DoUP and DoWg. An interesting finding is that the speed of the algorithm can be improved by processing additional information. Generally we note that the runtime of the MHT is directly proportional to the number of considered hypotheses.

TABLE 3
FM and CW - Tracking results for B01

Results only for NoCor	Start of track [ping]	End of track [ping]	Total Number of tracks
FM	54	146	66
FMCW DoUp	50	146	55
FMCW DoWg	51	144	44

1) Results for the modified data set A01: As expected the exploitation of CW information results for A01 in a decrease of the number of false tracks. For the modified data set of A01 we test whether, under these conditions, it is possible to lower

TABLE 4

FM AND CW - TRACKING RESULTS FOR A01

Results only for NoCor	Start of track [ping]	End of track [ping]	Total Number of tracks
FM	15	88	69
FMCW DoUp	12	88	17
FMCW DoWg	13	88	37

the SNR of E/R detection and still find the algorithm capable of generating only a reasonable number of false tracks. But

TABLE 5

DOUP - TRACKING RESULTS FOR THE MODIFIED DATA SET OF A01

Results only for NoCor	Start of track [ping]	End of track [ping]	Total Number of tracks
FMCW DoUp	13	37	20
	45	87	

in comparison to the processing of the original data set we observe a worse tracking performance, see Table 5. The track is terminated earlier and also fragmentized. This is caused by a lower P_D in the tracking inputs. The fragmentation coincides with the region, in which we note some missed detections due to Noise. Additionally, tracking performance is influenced by the value of the false alarm density (8), which increases with the number of considered contacts.

E. Results for variable probability of detection

The large latency in B01 requires some improvements. At best, we need 50 pings to extract the target (FMCW DoUP). The reasons are of course the missed detections in the beginning, whilst the probability of detection has been set equally to 0.5 during the whole run and for each S/R pair. In this section we discuss the effect of a variable probability of detection (SNRPD) dependent on the modeled SNR in Fig. 5. Table 6 shows the results. The track is already extracted during ping 20 and 28. It is terminated when all three receivers miss detection and starts again at ping 48; at least this is six pings earlier than in the standard approach. For A01 we use the Noise Level and the Transmission Loss

TABLE 6

SNRPD - TRACKING RESULTS FOR B01

Results only for NoCor	Start of track [ping]	End of track [ping]	Total Number of tracks
FM	54	146	66
FM SNRPD	20	28	63
	48	146	

and Ezio Baglioni to model the SNR, see Fig. 8. We only show tracking results for the modified data set and the FMCW Doppler Update method. By embedding the knowledge about the SNR in the tracker we get rid of the fragmentation, but we also observe a worse behavior in the beginning and in the end than with the fixed P_D, see Table 7 . These results show that if we are able to predict missed detection this knowledge will help the tracker to become more robust. More effort has to be invested.

TABLE 7

SNRPD - TRACKING RESULTS FOR A01

Results only for DoUP Cor	Start of track [ping]	End of track [ping]	Total Number of tracks
FMCW	13	37	20
	45	87	
FMCW SNRPD	21	87	28

V. CONCLUSION

Extending the MHT strategy to incorporate deterministic and stochastic a priori knowledge seems to be a viable way towards a robust, precise and real-time capable multistatic tracking algorithm. Several extensions have been implemented and evaluated by applying them to real data sets. Further evaluation is planned, using more available data sets from the same cruises, preDEMUS'06 and SEABAR 07.

ACKNOWLEDGEMENTS

This work was made possible through collaboration between NURC, a NATO Research Centre and FGAN-FKIE (DEU). The authors would like to thank Doug Grimmet, Ozer Eroglu, Ezio Baglioni and Kathrin Seget for discussion and support.

REFERENCES

[1] R. J. Ulrick, *principles of underwater*. McGraw-Hill Education; 2Rev Ed, 1976.

[2] H. Cox, "Fundamentals of active sonar," *Underwater Acoustic data Processing*,Y.T. Chan (ed.),pp. 3-24, 1989.

[3] W. Koch, J. Koller and M. Ulmke, "Ground target tracking and road map extraction", *ISPRS Journal of Photogrammetry & Remote Sensing*, vol. 61, pp. 197 - 208, 2006

[4] G. van Keuk, "Sequential track extraction", *IEEE Transaction on Aerospace and Electronic Systems*, vol. 34, pp. 1135-1148, 1998

[5] S. J. Julier and J. K. Uhlmann, "Unscented Filtering and Nonlinear Estimation," *Proceeding of the IEEE*, vol. 92, no. 3, 2004

[6] R. Klemm and W. Koch, "Ground target tracking with STAP radar: selected tracking aspects", *Principles of Space Time Adaptive Processing*, 2002

[7] M. Daun, W. Koch and R. Klemm, "Tracking of ground targets with bistatic airborne radar", *sumbmitted for Radar Conference*, 2008

[8] F.R. Martin-Lauzer, M. Stevenson, S. Jespers, F. Ehlers, "Coalition of ASW Sensors" *Defence Technology Asia*, Singapore, March 2007.

[9] S. S. Blackman and R. Populi, "Design and analysis of modern tracking systems "*,Artech House Radar Libary*, 1999

[10] Y. Bar-Shalom and X.-R. Li, "Multiarget-multisensor tracking: Applications and Advances"*,Artech House Radar Libary*, 1995